NEOPLASIA
www.neoplasia.com

Volume 10 Number 7 July 2008 pp. 687–696 687

A Splice Variant of HER2 Corresponding to Herstatin Is Expressed in the Noncancerous Breast and in Breast Carcinomas[1]

Triantafyllia Koletsa*, Ioannis Kostopoulos*, Elpida Charalambous*, Barbara Christoforidou†, Eleni Nenopoulou* and Vassiliki Kotoula*

*Department of Pathology, Aristotle University Medical School, Thessaloniki, Greece; †Theageneion Cancer Hospital, Thessaloniki, Greece

Abstract

Herstatin (HST) is an alternatively spliced HER2 product with growth-inhibitory properties in experimental cancer systems. The role of HST in adult human tissues and disease remains unexplored. Here, we investigated HST expression at the mRNA and protein (immunohistochemistry [IHC]) level in parallel with parameters reflecting HER activation in 187 breast carcinomas and matched noncancerous breast tissues (NCBT). Noncancerous breast tissues demonstrated the highest HST/HER2 transcript ratios corresponding to a few positive epithelial and stromal cells by IHC. Although HST/HER2 transcript ratios in tumors were inversely associated with HER2 IHC grading ($P = .0048$ for HER2 IHC-1+ and $P = .0006$ for HER2 IHC-2+ *vs* HER2-negative tumors), relative HST expression within the same tumor/NCBT system remained constant. HST/HER2 ratios did not predict the presence of HST protein, which was found in 46 (25%) of 187 tumors. A subgroup of HER2 IHC-3+ tumors exhibited high HST/HER2 transcript ratios, strong HST protein positivity, and cytoplasmic phospho–Akt/PKB and $p21^{CIP1/WAF1}$ localization. In conclusion, HST may act as a paracrine factor in the adult breast. Because HST is described as an endogenous pan-HER inhibitor, the presence of this protein in breast carcinomas may portent the inefficiency of exogenous efforts to block HER2 dimerization, whereas its absence may justify such interventions.

Neoplasia (2008) 10, 687–696

Introduction

Two decades ago, HER2/neu overexpression in approximately 30% of breast carcinomas was first associated with adverse disease prognosis [1], p185-HER2 overexpression proved transforming and tumorigenic for cultured mouse fibroblasts [2], whereas a specific anti–185-HER2 antibody showed antiproliferative activity *in vitro* [3]. This basis provided the rationale for the development [4] and clinical establishment of trastuzumab in the treatment of breast cancer [5–7]. However, resistance to trastuzumab is still the case in approximately 50% of HER2-amplified/overexpressing tumors [5,6]. To overcome resistance and to overall improve clinical outcome in targeted breast cancer treatment, further combined use of anti-HER antibodies and kinase inhibitors has been proposed [8–11]. One such anti-HER monoclonal antibody is 2C4 (pertuzumab) [12], which was designed to inhibit HER2-dependent signaling in both HER2 low- and high-expressing tumors. Pertuzumab binds HER2 extracellular domain (ECD) at an area other than trastuzumab and inhibits HER2 dimer formation and, hence, activation [13].

Interestingly, dominant-negative HER2 regulators with pertuzumab-like properties are produced endogenously as well, in fact, as alternatively spliced products of the *HER2* gene itself. At least two such molecules have been identified and described as p68-HER2 and p100-HER2 [14,15]. p68-HER2, the most advanced studied molecule of these two, was initially called herstatin (HST) [15] and later dimercept [16]. Herstatin mRNA is an alternatively spliced *HER2*

Abbreviations: HST, herstatin; NCBT, noncancerous breast tissue; IHC, immunohistochemistry; FFPE, formalin-fixed paraffin-embedded

Address all correspondence to: Vassiliki Kotoula, MD, PhD, Aristotle University, School of Medicine, Department of Pathology, University Campus, 54006 Thessaloniki, Greece. E-mail: vkotoula@auth.gr

[1]This work was supported in part by PENED-03/583, a research grant from the General Secretariat for Research and Technology (Ministry of Development, Athens, Greece).
Received 20 February 2008; Revised 26 April 2008; Accepted 28 April 2008

DOI 10.1593/neo.08314

product retaining intron 8; the translated protein is identical to HER2 ECDI and most part of ECDII with a unique carboxy-tail sequence substituting for ECDIII [15]. With this tail, HST specifically binds HER2 ECDII [17] in a way similar to pertuzumab [13], whereas it also binds epidermal growth factor receptor (EGFR) and HER4, and less insulin-like growth factor 1 receptor [18]. Herstatin is a soluble protein, because it lacks a transmembranous domain and it can be secreted from the cells it has been produced [15]. Herstatin specifically prevents HER2/HER3 and HER2/EGFR dimer phosphorylation by disrupting dimers formed with HER2 [19], whereas it inhibits transforming growth factor alpha– and EGF-stimulated proliferation [20] and heregulin-dependent growth in breast cancer cells [21]. The same effects have correspondingly been described for pertuzumab [13,22,23]. In the experimental therapeutic context, HST expression in glioblastoma cell implants in female rats prevented intracranial tumor formation [24].

Currently, it is not known whether HST is expressed in adult human tissues. If HST serves as an endogenous pan-HER "antibody," cancers would be expected to lack HST expression. If cancers express HST and still thrive, native HST production might not be effective in inhibiting HER signaling. In this study, we investigated HST mRNA expression and protein presence in breast carcinoma tissues in parallel to their normal counterparts, in association with HER2 IHC status and parameters reflecting downstream effects of HER activation, such as phosphorylation of Akt/PKB and compartmentalization of $p21^{Cip1/WAF1}$. The latter two parameters were chosen on the basis of *in vitro* data showing that activated HER2 dimers on the cell membrane exert their cell growth effects in part through Akt/PKB phosphorylation, which then phosphorylates and prevents the nuclear translocation of the cell cycle inhibitor $p21^{Cip1/WAF1}$ [25]. At this state, both proteins are located in the cytoplasm. At the tissue level, the subcellular localization of phosphorylated Akt at Ser473 (pAkt) as detected by immunohistochemistry (IHC) seems to be related with poor prognosis and response to therapy in breast cancer [26,27]. HER2 overexpression is frequently associated with pAkt [28,29] and with cytoplasmic $p21^{Cip1/WAF1}$, which may be used as a predictor of response to trastuzumab [30,31]. Although tested on different cell systems, both HST [20] and pertuzumab [23] were able to block Akt/PKB phosphorylation.

In this study, we asked whether HST, the endogenous analogue of pertuzumab, is produced in the adult breast and in breast carcinomas and, if yes, in which association to established disease and to HER2 activation parameters. The study was performed on routine pathology material, whereby special care was paid on sampling from cancer and normal-appearing breast tissue. Real-time polymerase chain reaction assays were designed for the specific detection of HST and the corresponding area of HER2 transcripts, whereas a monoclonal antibody that specifically targets the carboxy-tail of HST was used for the *in situ* detection of this protein. We found that HST transcripts and protein are expressed in the noncancerous breast, where this molecule may have a paracrine action and interfere with tissue homeostasis. In breast carcinoma tissues, HST mRNA levels do not predict for the presence of the corresponding protein in 75% of cases, indicating that cancer cells are protected by some regulatory mechanism from the growth-inhibitory effects of this molecule. Most importantly, however, if 25% of breast carcinomas grow in the presence of this endogenous pan-HER inhibitor, which is produced in high amounts in some cases with adverse prognostic parameters (HER2 overexpression, activated Akt/PKB, and blocked $p21^{CIP1/WAF1}$), then it remains questionable whether these cancers would benefit from exogenous attempts to disrupt HER dimerization.

Materials and Methods

Tissues

Previously diagnosed formalin-fixed paraffin-embedded (FFPE) breast carcinoma tissues from 187 female patients were retrieved from the archives of the Department of Pathology, School of Medicine, Aristotle University, and from the Laboratory of Pathology, Theagenion Cancer Hospital, according to the Declaration of Helsinki principles and institutional review board policies. Patient and tumor data are presented in Table 1. The term *NCBTs* (noncancerous breast tissue) is used instead of *normal* throughout this study for morphologically normal tissue adjacent to breast carcinomas. These structures have recently been shown not to have undergone substantial changes in their gene expression profile when compared to normal breast tissue obtained from mammoplasty specimens [32]; hence, NCBT is considered safe to use in comparative studies of tumor gene expression profiles.

Tissue Microarray Construction

Low-density tissue microarrays (TMAs; 14–16 cases per array) were constructed with the Beecher manual tissue arrayer (Beecher Instruments, Sun Prairie, WI). Seven cores from different areas in the same breast carcinoma, along with three cores from matched noncancerous breast tissue, were included from each case (core diameter, 0.6 mm). Cores from normal skin and colon adenocarcinomas were also included as controls and for block orientation.

RNA Extraction and Reverse Transcription

Tissue fragments were manually microdissected from cancerous and NCBT areas corresponding to those included in the TMA cores in 70 cases. These cases were selected on the basis of the content of at least one normal-appearing ductal unit and surrounding epithelial

Table 1. Patient Data, Tumor Histologic Diagnosis, and Conventional Markers.

Age	<50 years	49	26.2%
	>50 years	106	56.7%
	Unknown	32	17.1%
Tumor size	<1 cm	5	2.7%
	>1 cm	128	68.4%
	Unknown	54	28.9%
Lymph nodes	0	25	13.4%
	1	16	8.6%
	>1	42	22.4%
	Unknown	104	55.6%
Histologic diagnosis	NOS	147	78.7%
	Lobular	17	9.1%
	Medullary	3	1.6%
	Mucinous	7	3.7%
	Anaplastic/squamous	1	0.5%
	Mixed subtypes	9	4.8%
	Mixed	3	1.6%
Tumor grade	I	10	5.4%
	II	73	39%
	III	104	55.6%
ER	Negative	73	39%
	Low	27	14.5%
	Medium	39	20.9%
	High	48	25.6%
HER2	Negative	55	29.4%
	1+	59	31.6%
	2+	40	21.4%
	3+	33	17.6%

tissue that could be safely, manually microdissected without contamination of cancer infiltrates. RNA was extracted on overnight proteinase K digestion with TRIZOL-LS (Invitrogen, Paisley, UK).

Reverse Transcription–Polymerase Chain Reaction for the Detection of HST and HER2 Transcripts

Random hexamers and Superscript II with an additional RNase H (all from Invitrogen) incubation step were used for first-strand cDNA synthesis. Primers, probes, and the rationale for protocol designing are shown in Figure 1*a*. Of note, the HER2 product with spliced intron 8 does not necessarily correspond to the fully spliced mRNA from NM_004448.2, because more splice variants have been described concerning regions corresponding to or flanking the transmembranous domain [14,33]. Initial screening of all samples for HST and HER2 transcripts was performed with simple reverse transcription–polymerase chain reaction (RT-PCR) and Ready-To-Go PCR beads (Amersham, Piscataway, NJ). The 165-bp HST product (Figure 1*b*) was validated by sequencing. For relative quantification with real-time PCR, HST, HER2, and ACTB (*β-actin*, housekeeping gene) targets were amplified with the corresponding TaqMan probes during 45 cycles at 95°C – 15 seconds at 60°C – 1 min in an ABI7500 sequence detection system (Applied Biosystems, Biosolutions, Athens, Greece). Standard curves for HST, HER2, and ACTB showing acceptable PCR efficiency for all targets were obtained by using a cDNA template from an HER2 1+ breast carcinoma. Standard dilutions were prepared at 100, 50, 5, and 0.5 ng of cDNA per reaction. Corresponding slopes of the curves were as follows: ACTB, −3.4; HER2, −3.6; and HST, −3.4; and corresponding R^2 values were as follows: ACTB, 0.99; HER2, 0.99; and HST, 0.98.

Relative quantification of HST *versus* ACTB and HER2 in tumor *versus* pooled and separately paired NCBT samples was assessed with the SDS v1.3 software, which uses the $2^{-\Delta\Delta Ct}$ method [34]. In addition, the $2^{-\Delta Ct}$ method [34] was used to assess HST/HER2 transcript ratios in the same sample on the basis of equal efficiencies for the amplification of PCR targets. Samples were normalized to contain approximately 50 ng of cDNA per reaction. The reading threshold was set at 0.08, and the relative quantification minimum/maximum confidence interval was at 99.9%. Runs were repeated at least twice for all samples.

Immunohistochemistry for HST

The CW001 monoclonal antibody (Upstate Biotechnology, Lake Placid, NY), which has been raised against the characteristic HST protein carboxy-tail, was used at a 1:75 dilution. Antigen retrieval was accomplished with proteinase K for 5 min at room temperature. Binding was developed with the Envision system (DAKO, Carpinteria, CA) and visualization with diaminobenzidine (DAKO). Negative controls to assess specificity of staining included (i) preabsorption of CW001 with recombinant HST protein (generously supplied by BioVendor, Brno, Czech Republic) in PowerBlock, (ii) addition of a universal antimouse-negative control antibody (DAKO), and (iii) omission of primary antibody during overnight incubation. The IHC protocol was standardized on whole-breast sections including tumor and normal areas.

Immunohistochemistry for HER2-Related Targets

Immunohistochemistry for estrogen receptor alpha (ERα) and for HER2 intracellular domain (HercepTest; DAKO, Glostrup,

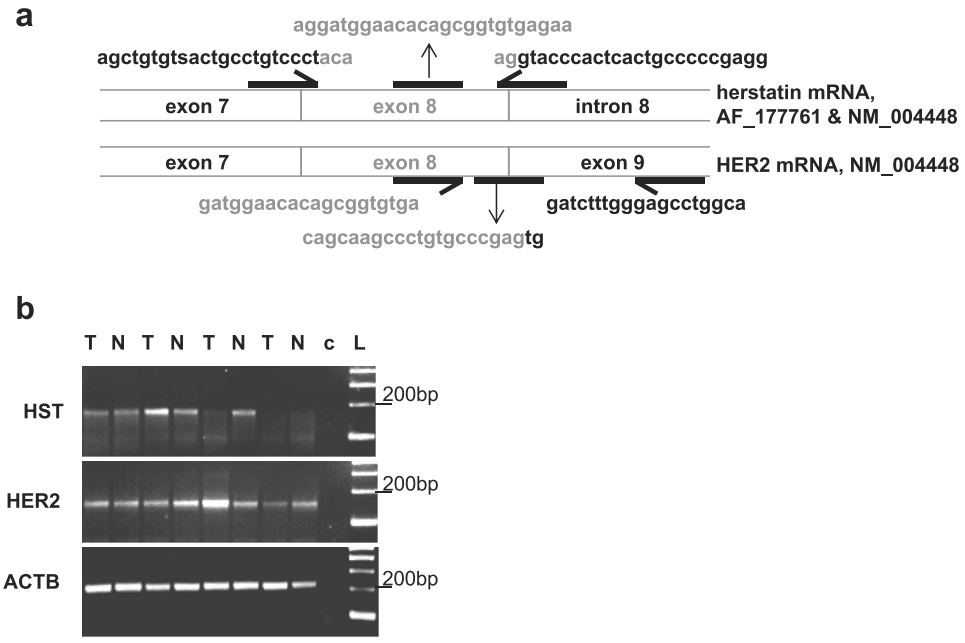

Figure 1. Design of the real-time PCR assays that were used for the investigation of HST expression in breast carcinomas. (a) Specific primers and probes were designed for the detection of HST (165-bp product retaining intron 8) and HER2 (150-bp product lacking intron 8, probably corresponding to HER2 receptor) mRNA targets. The sense HST primer includes an S corresponding to the silent G/C mismatch in exon 7 (AF_177761 and NM_004448), which in two of three sequenced cases proved to be a G. Theoretically, a 424-bp product corresponding to HST transcripts would coamplify with the wild type HER2 target; this, however, could not be observed in the FFPE samples. Sequences are shown in 5′–3′ sense direction. (b) Representative RT-PCR results for matched NCBT/tumor pairs are shown. Specific HST products are detected in the presence of HER2.

Denmark) was performed in an automated system according to standard diagnostic protocols. Clone MIB-1 (DAKO, Carpinteria, CA) was used for the evaluation of tumor proliferation status. To assess HER activation status, monoclonal antibodies against phosphorylated Akt/PKB (pAkt-S473; Cell Signaling Technologies, Beverly, MA) and $p21^{CIP1/WAF1}$ (DAKO, Carpinteria, CA) were used. A tryptase staining had to be used for the validation of mast cells.

Immunohistochemistry Evaluation

There is currently no reference on how to evaluate HST IHC on naive tissues. Staining was evaluated under medium (×200) and high (×400) power. Tumors were considered negative when no HST-specific intracytoplasmic staining was observed in the neoplastic cells on any core. A cutoff of 25% was used to evaluate low and high HST positivity, because, although most positive tumors exhibited HST-specific staining in single cells (<25%, low HST), in some tumors, strong staining in 30% to 70% (>25%, high HST) of neoplastic cells was repeatedly observed. The status of Akt/PKB phosphorylation was evaluated as negative (absence of staining), nuclear (exclusively nuclear staining in >50% of cells), and positive (staining in the cytoplasm only, or in both cytoplasm and nuclei). Staining for $p21^{CIP1/WAF1}$ was evaluated as negative (absence of staining), nuclear (presence in the nucleus only), and cytoplasmic (exclusively cytoplasmic or nuclear and cytoplasmic). MIB-1 labeling index was assessed as the percentage of positive tumor cells in all cores under medium power (×200). For the assessment of each tumor, staining in all cores was assessed. If less than five of seven cores were available on TMA sections per tumor, cases were considered as inadequately represented and were not further evaluated.

Statistics

Statistical analyses were performed with the SPSS software (v14; SPSS, Inc, Chicago, IL). Spearman's Rho was used to correlate relative quantification results. The Mann-Whitney test was used for the comparison of relative quantification values *versus* IHC results; the same test was used to evaluate IHC results between subgroups of markers, whereas the Kruskal-Wallis test was used to evaluate the overall impact of IHC staining profiles among qualitative markers.

Results

HST mRNA Is Expressed in NCBT and Breast Carcinomas

All 70 tumors but only 63 of 70 NCBT samples yielded amplifiable templates for PCR. Herstatin transcripts were identified by simple RT-PCR in 58 (92%) of 63 NCBT and in 55 (78.6%) of 70 tumor samples (Figure 1*b*), always in the presence of HER2 transcripts. Reliable amplification curves (cycle threshold [C_t] < 40) were detected with real-time PCR in 63 (100%) of 63 amplifiable NCBTs and in 61 (92.9%) of 70 tumor samples.

HST Expression in Breast Carcinomas Is Related to HER2 mRNA and Protein Expression

Relative HER2 values *versus* ACTB were fairly constant among NCBTs, ranging from 0.2043 to 1.399 (mean ± SD 1.017 ± 0.5285), comparable to previous reports [35]. By contrast, relative HST values *versus* ACTB varied extensively among NCBTs (>3 log orders); hence, all relative quantification analyses were assessed in matched tumor/NCBT pairs (n = 61). In these sample pairs, relative

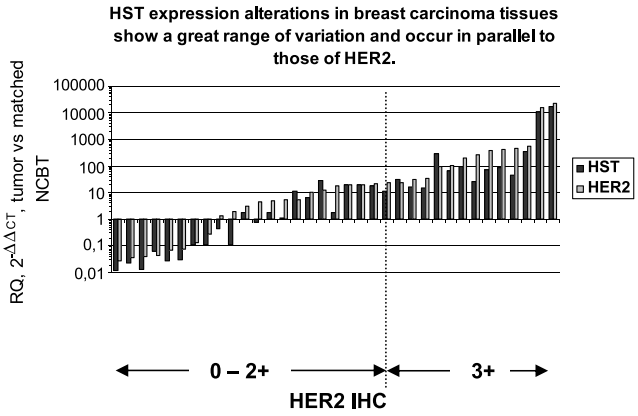

Figure 2. Both HST and HER2 are overexpressed in HER2 IHC 3+ tumors. Relative HER2 and HST expression in tumor *versus* matched NCBT pairs with ACTB as the endogenous reference is shown in a series of 24 cases. Herstatin relative quantification values ranged from 0.012 to 16,949.78 (mean ± SD, 428.21 ± 2413.54), in a similar log range to those of HER2 (range, 0.027–23469.40; mean ± SD, 640.86 ± 3335.93). Relative HER2 and HST expression values *versus* ACTB strongly correlated with HER2 IHC and were significantly higher in HER2-overexpressing tumors than in all other HER2 grading categories (Mann-Whitney, $P < .00001$ for both HER2 and HST).

HST expression positively correlated to that of HER2 (Spearman's rank test, $P < .00001$), whereas both relatively high HST and HER2 expression were associated with HER2 IHC (Figure 2). Relative HST/HER2 ratios within the same tumor/NCBT milieu, however, did not differ on HER2 IHC grading ($P = .531$).

Individual samples expressed less HST than HER2 transcripts, because HST/HER2 ratios were always <1 in the same sample (Figure 3). HST/HER2 ratios in individual tumor samples varied according to HER2 IHC grading.

HST/HER2 ratios were generally higher in NCBTs than in the matched tumors (Figure 3*a*), but this did not reach statistical significance. However, NCBTs adjacent to HER2 IHC grade 3+ tumors expressed very low HST levels in half the cases of this tumor category. Although individual tumor groups are small (Figure 3*a*) and the analysis is prone to statistic errors, these results show that HST/HER2 ratios in tumors differed according to HER2 grade but not according to HST immunopositivity. In addition, these results further support that HST/HER2 ratios among tumor/NCBT systems were independent of HER2 IHC grading, as mentioned previously. This can be particularly observed in HER2-overexpressing cases, where high HST/HER2 ratios in tumors were accompanied by low HST/HER2 ratios in the corresponding NCBTs and *vice versa* (Figure 3*a*).

HST Protein Detection by IHC and Its Association with Relative HST Expression

Currently, there are no reference data on HST protein presence in naive tissues, hence an established positive reference was not available. Herstatin staining proved specific, because besides conventional negative controls, incubation with the recombinant HST protein after preabsorption with the CW001 anti-HST antibody resulted in the disappearance or marked fainting of staining (Figure 4, *b* and *d*).

a

HER2 IHC grading is related to HST/HER2 transcript ratios in tumors, whereby two subgroups are distinguished in HER2-3+ graded tumors.

		HST/HER2 in tumors			HST/HER2 in NCBT		
	n	mean	SD	p#^	mean	SD	p#^
		0,0137	0,0143		0,0416	0,1176	
HER2 IHC							
negative	25	0,02	0,0031		0,0128	0,0021	
1+	20	0,0075	0,0019	0,0048*	0,0526	0,0255	
2+	5	0,0045	0,0007	0,0006*	0,1601	0,151	
3+ / HSTlow	8	0,0048	0,0029	0,0025	0,0781	0,0921	0,0019
3+ / HSThigh	5	0,0277	0,0166		0,0008	0,0006	
HST IHC (tumors)							
negative	34	0,0123	0,0134		0,0653	0,1519	0,0118**
positive	29	0,0156	0,0154		0,0101	0,0112	

Footnotes:
#: only statistically significant results are shown;
^: Mann-Whitney exact 2-sided significance;
* : comparisons against HER2 IHC negative cases;
** : corresponds to very low HST expression in NCBTs matched to $HER2_{high}/HST_{high}$

b

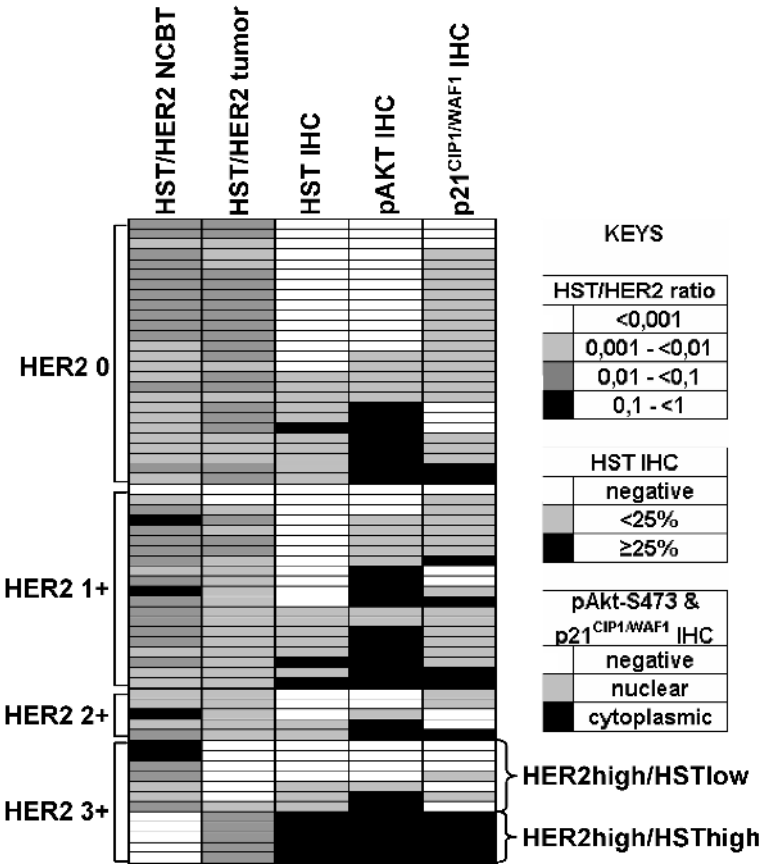

Figure 3. HST/HER2 ratios within the same tumor distinguish two subgroups in HER2-overexpressing tumors with specific AKT/PKB activation profiles. (a) Mean values and statistically significant differences in the different tumor subgroups show that the ratio of HST *versus* HER2 transcripts declines with increasing HER2 expression. However, there is one subgroup of HER2 3+ tumors that overexpress HST. The NCBT counterparts of these tumors practically lack HST expression. (b) Artificial heatmap showing the associations of HST/HER2 ratios in tumors and matched NCBTs with HST immunopositivity, as well as with AKT/PKB activation profile. Cases have been grouped according to their HER2 status as assessed with IHC. The highest HST/HER2 ratios were observed in NCBTs and in HER2 IHC-negative or grade 3+ tumors. HST/HER2 ratios were significantly low in HER2 IHC grade 1+, 2+, and in the remaining HER2 IHC grade 3+ tumors. Note the difference in the total profile between $HER2_{high}/HST_{low}$ and $HER2_{high}/HST_{high}$ tumors.

Herstatin protein was observed mainly in the cytoplasm, seldom on cell membranes, and never in the nuclei, while it was also present in the cytoplasm of stromal mast cells and as fine granules diffusely in the stroma (Figure 4, *a* and *c*), in line with the soluble nature of this protein [15]. Herstatin-positive mast cells were observed in all NCBTs, except for those in the neighborhood of $HER2–3+/HST_{high}$ tumors. Positive mast cells were also observed in the stroma of 80 (42.7%) of 187 tumors, unrelated to HST staining in tumor cells.

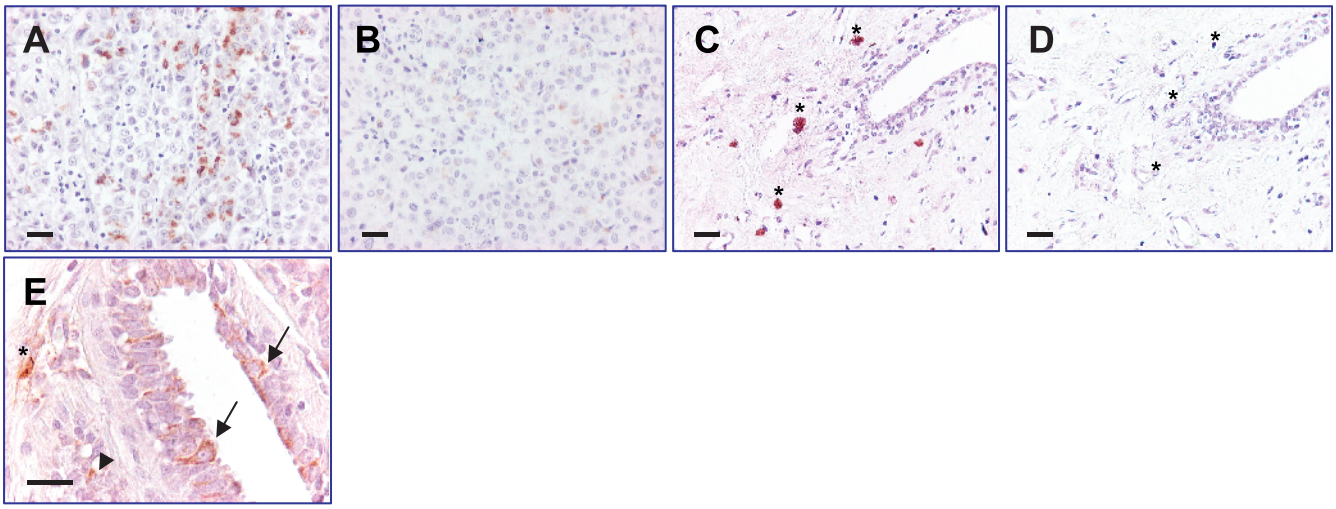

Figure 4. HST protein detection by IHC. (a–d) Testing on tissue sections for the specificity of the anti-HST antibody (CW001 clone, staining in panels (a) and (c)) with preabsorption of the antibody with recombinant HST protein (mass ratio of 1:5, overnight incubation at 4°C, markedly reduced or absent staining in (b) and (d)). (a and b) Same area of a HER2 IHC-2+ breast carcinoma; (c and d) same area of the corresponding NCBT. Herstatin staining is specific in the cytoplasm and perinuclear area of tumor cells (a) and in mast cells mostly observed around noncancerous breast elements (c). (e) Staining for HST protein in the cytoplasm of NCBT is faint but specific, as observed under high magnification. *Asterisks* in panels (a)–(e) point at mast cells. *Arrows* in panel (e) point at positive epithelial cells; *arrowhead*, positive endothelial cell. Scale bars, 50 μm.

In NCBTs, faint HST staining was detected in ductal epithelial cells, some capillary endothelia, and seldom in lobular units and myoepithelial cells (Figure 4*e*).

Although HST transcripts were found in most tumor tissue samples, HST protein could be detected in the neoplastic cells of only 46 (24.6%) of 187 tumors with immunopositivity usually confined to <25% of tumor cells (36/46 [78.2%] HST-positive cases). Herstatin-positive cells were distributed evenly among negative ones without focal accumulation, as observed during staining standardization on whole sections. The HST positivity pattern in tumors was comparable to NCBTs, but the staining intensity in tumors was stronger (Figure 4*a*). Herstatin immunopositivity in tumor cells was generally not associated with tumor HST/HER2 ratios (Table 2). The only cases where HST IHC fully corresponded to HST/HER2 ratios were $HER2_{high}/HST_{high}$ tumors (P = .0020 between the two HER2 IHC-3+ subgroups). In these cases, HST/ACTB ratios and HST relative expression *versus* matched NCBTs were significantly high (P = .0283).

HST Immunopositivity Is Associated with HER2 Status and Cytoplasmic Localization of Phosphorylated Akt/PKB and p21$^{CIP1/WAF1}$

Statistically significant associations of the IHC results from this study are presented in Table 2, *a–c*. Herstatin positivity in tumor cells was not associated with patient age, ER and lymph node status, tumor size and grade, MIB-1 labeling index, whereas it was strongly associated with HER2 protein expression and Akt/PKB phosphorylation, and marginally with cytoplasmic localization of $p21^{CIP1/WAF1}$ (Table 2 *a*). The lowest incidence of HST-positive tumors was observed in the HER2 IHC-2+ group (13.5%) and the highest in the group of HER2-overexpressing tumors (50%, P = .0015). In addition, whereas HST positivity was observed in only 10.5% of tumors without detectable Akt/PKB activation, it was present in 37.5% of tumors with cytoplasmic pAkt-Ser473 localization ($P_{Mann\text{-}Whitney}$ = .0001).

HER2 grading was unrelated to MIB-1, inversely associated with ER status (P = .0009), as already established, and showed one-sided association with cytoplasmic p21 and pAkt-Ser473 (Table 2 *b*). In turn, pAkt-Ser473 was overall significantly associated with the expression of $p21^{CIP1/WAF1}$ (Table 2 *c*), especially in terms of cytoplasmic $p21^{CIP1/WAF1}$ localization ($P_{Mann\text{-}Whitney}$ = .0004). Interestingly, all $HER2–3+/HST_{high}$ tumors that showed >25% HST immunopositivity were also positive for cytoplasmic pAkt-S473 and $p21^{CIP1/WAF1}$ (Figures 3*b* and 5).

In comparison, when present, pAkt-S473 was localized in the nuclei of NCBT epithelial cells; $p21^{CIP1/WAF1}$ was also observed in the nucleus, although very rarely.

Discussion

Herstatin a soluble truncated HER2 variant that acts as a pan-HER inhibitor, has been considered as a growth regulator during normal development, because it is expressed in fetal kidney and liver tissues [15], whereas its interference with HER dimer activation may disturb proper hart valve formation [36] and impair cartilage and bone development [37] in experimental models. In this study, we show that HST mRNA and protein are expressed in the noncancerous breast, in areas adjacent to breast carcinomas. In normal epithelial cells, low relative HER2 levels are expressed [35] and correspond to approximately 2 to 4×10^4 HER2 molecules per cell [38] that translate into negative or faint HER2 immunostaining. According to the high HST/HER2 ratios in most NCBTs (up to 25% of HER2 transcripts), the number of HST transcripts described here would then be approximately 200 per cell. It seems that at the tissue level, HST is produced by few epithelial and endothelial cells, whereas, as a soluble protein [15], it may also accumulate in mast cells, suggesting a paracrine action as well. This characteristic pattern of HST expression in NCBTs might contribute to the normally effective endogenous HER-inhibition system

Table 2. HST Immunopositivity Strongly Correlates with pAkt But Only Marginally with $p21^{CIP1/WAF1}$ Status (*a*).

(*a*)	Total* (%)	HST			$P^{\dagger}$
		Negative	<25%	≥25%	
HER2					
Negative	55/187 (29.4)	45	9	1	
1+	59/187 (31.6)	47	10	2	**.0066** (HER2 *vs* HST)
2+	40/187 (21.4)	35	5	0	.2778 (HST *vs* HER2)
3+	33/187 (17.6)	17	9	7	
pAkt					
Negative	67/169 (39.6)	60	7	0	**.0005** (pAkt *vs* HST)
Nuclear	38/169 (22.5)	25	12	1	**.0002** (HST *vs* pAkt)
Cytoplasmic	64/169 (37.9)	40	15	9	
$p21^{CIP1/WAF1}$					
Negative	54/169 (32)	45	7	2	**.046** (HST *vs* p21)
Nuclear	77/169 (45.6)	58	13	6	**.0639** (p21 *vs* HST)
Cytoplasmic	38/169 (22.4)	23	8	7	

(*b*)	Total* (%)	HER2				$P^{\dagger}$
		Negative	1+	2+	3+	
pAkt						
Negative	71/173 (41)	21	15	27	8	**.0002** (HER2 *vs* pAkt)
Nuclear	38/173 (22)	10	15	5	8	.8309 (pAkt *vs* HER2)
Cytoplasmic	64/173 (37)	22	21	5	16	
$p21^{CIP1/WAF1}$						
Negative	57/173 (33)	20	12	17	8	**.0077** (HER2 *vs* p21)
Nuclear	77/173 (44.5)	25	24	15	13	.1723 (p21 *vs* HER2)
Cytoplasmic	39/173 (22.5)	6	16	5	12	

(*c*)	Total* (%)	pAkt			$P^{\dagger}$
		Negative	Nuclear	Cytoplasmic	
$p21^{CIP1/WAF1}$					
Negative	57/170 (33.5)	31	11	15	**.0016** (pAkt *vs* p21)
Nuclear	76/170 (44.7)	30	19	27	**.0011** (p21 *vs* pAkt)
Cytoplasmic	37/170 (21.8)	7	8	22	

HER2 status in (*a*) and (*b*) is strongly associated with all parameters tested but only one-sided, whereas cytoplasmic pAkt (*c*) strongly correlates with cytoplasmic $p21^{CIP1/WAF1}$.
*Total number of cases for each marker pair vary due to availability of tissue on TMAs.
†Kruskal-Wallis test significance (asymptotic, one-sided); for each set of parameters, *P* is presented in both directions. Significant associations are in bold.

[39], because there is a local need for HER inhibition in differentiating ductal epithelia [40].

HST/HER2 transcript ratios in tissues were comparable but generally lower than those described in cell lines [15], a result probably due to tissue cell heterogeneity. HST/HER2 transcript ratios in breast tumors inversely correlated with HER2 protein expression. However, HST/HER2 ratios of 2% in HER2-negative, 0.8% in HER2 – IHC 1+ and 0.5% in HER2 – IHC 2+ tumors reflect an almost constant *niveau* of HST expression in tumors without overt HER2 overexpression, given the corresponding rise in HER2 transcripts. The trend toward equilibrium of HST/HER2 expression was further noticed among the entire group of 63 tumor/NCBT matched pairs examined, including tumor/NCBT pairs in HER2-overexpressing cases. This finding may indicate that increased HST expression is prevented in breast tissues in order not to disturb vital for homeostasis growth factor signaling through the HER receptor system [41] as would be expected from the high affinity with which functional HST binds to its targets [15,18–21].

Unlike the situation in cell lines [15], HST mRNA levels in tumors were, in most cases, not predictive of HST protein presence. This was more pronounced in $HER2_{high}/HST_{low}$ tumors, where values of 0.5% would evidently correspond to a higher number of molecules than that observed in NCBTs. The possibility that few HST-positive cells might have been missed due to poor representation of tumor tissue on the TMA cores seems unlikely, because multiple areas from each tumor were examined, whereas, as described, HST-positive cells were distributed throughout the tumor tissue. Whether HST mRNA does not reach the translation point due to posttranscriptional inhibitory interference or whether this soluble protein is produced but escapes to the circulation remains unknown. About the latter option, circulating HER2 ECD molecules are currently routinely measured (for example, [42–45]) by an FDA-approved ELISA system [46] that was patented back in 1991 [47]. The system detects HER2 molecules of 95 to 115 kDa including the entire ECD, but it cannot distinguish whether these are produced by proteolytic shedding from the full-length receptor [48] or as translated proteins from alternatively spliced products [14,33], which could also escape into the circulation because they are soluble. All versions of this system have used two antibodies, NB-3 and TA-1, which

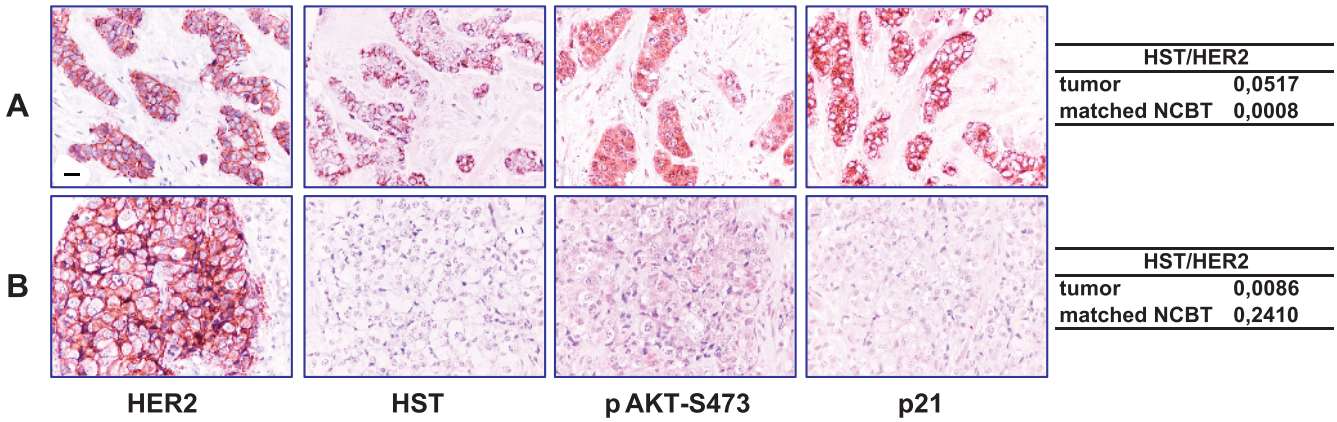

Figure 5. HST/pAKT/$p21^{CIP1/WAF1}$ profiles in HER2-overexpressing tumors. All photomicrographs are of the same magnification (scale bar, 50 μm). In the $HER2_{high}/HST_{high}$ tumor in panel (a), most neoplastic cells are positive for HST protein; pAKT and $p21^{CIP1/WAF1}$ are localized in the cytoplasm, whereas the HST/HER2 transcript ratios are high in the tumor and low in the adjacent NCBT sample. In the $HER2_{high}/HST_{low}$ tumor in panel (b), HST, pAKT, and $p21^{CIP1/WAF1}$ are not detected, whereas HST/HER2 transcript ratios in the corresponding tumor and NCBT samples are inverse in comparison to that observed in panel (a).

recognize different epitopes on HER2 ECD [47]. Because these epitopes have not been described, it cannot be excluded (unless proven otherwise) that circulating HST molecules are detected by this system as well. In this context, it seems worthy to assess the presence of HST in the circulation by HST-specific detection methods. Herstatin with its unique carboxy-tail represents, in fact, a rare example of a splice variant involved in a major signaling pathway for which specific antibodies can be raised, such as the one used in the present study.

Most unexpectedly, approximately 1/5 of HER2-overexpressing tumors were found to express relatively high HST/HER2 mRNA ratios and to be strongly positive for HST protein. In comparison, the NCBTs next to these tumors produced the lowest levels of HST encountered in this study, a finding further supporting a paracrine role for HST in breast tissue and, perhaps, a paracrine regulatory mechanism. This tumor group further exhibited a unique profile of strong cytoplasmic phospho–Akt/$p21^{CIP1/WAF1}$ protein positivity, which, in the presence of HER2 overexpression, has been associated with adverse prognosis in breast cancer and poor response to therapy [26–31,49–51].

In addition, a strong bidirectional association between HST protein and activated Akt/PKB was observed throughout the tumor series examined in this study. It must be noted that with the commonly used antibody for the demonstration of activated Akt/PKB with IHC, which was used here as well, it is possible to detect not only phosphorylated Ser473 on Akt1 but also the corresponding serines on Akt2 and 3. Hence, it is impossible to distinguish which Akt is phosphorylated. It is known that all three Akt isoforms, which may have distinct roles in cancer progression [52,53], are produced in breast cancer [54], where they have mainly prosurvival [55] and questionable cell migration effects [56]. The antibody used detects pAkt-S473 in the cytoplasm, cell membrane, and nucleus. Although the presence of pAkt in the nucleus may be important for cancer progression because it seems related to MDM2 phosphorylation and p53 inactivation [57,58], nuclear compartmentalization of pAkt may also be detected in normal breast epithelial cells, as we have observed here. Nevertheless, because the previously mentioned literature data on pAkt in breast cancer are based on the evaluation of cytoplasmic staining [26–31,50], we considered this subcellular localization of Akt/PKB as the prosurvival and poor prognosis indicator. The simultaneous presence of cytoplasmic $p21^{CIP1WAF1}$ and pAkt, which further suggests a growth advantage for the tumors [25,31,59], was also marginally associated with the presence of HST. Because HST has been described to block EGF/EGFR–induced Akt/PKB phosphorylation and proliferation *in vitro* [20], the previously mentioned findings could be interpreted as an attempt by the HST-positive cancer cells to block Akt/PKB phosphorylation. Anti-HER antibodies such as 2C4 or the newly developed Mab806 seem not to necessitate an active conformation of the receptor to achieve its internalization [60]. In our cases, no correlation was observed for HST *versus* membranous EGFR and EGFR-Y992; there was a vague association between HST and EGFR phosphorylation at Tyr1068 (our unpublished data). In all, however, the fact that tumors grow although they may express high levels of HST reflects the inefficiency of this molecule to inhibiting tumor growth *in vivo*.

Alternatively, strong cytoplasmic HST localization may indicate that this protein is impaired from exiting the cells by some as yet unknown mechanism and, hence, it cannot bind to the extracellular domain of HER receptors and exert its inhibitory action. If such an export-inhibitory regulation is proven for tumors with strong cytoplasmic HST, then these tumors might benefit from external HST administration.

Whether HST (or dimercept) will ever enter clinical trials, as previously observed [16,24], remains unknown, especially because the idea seems abandoned [61]. Published results from corresponding testing of its manufactured "analogue," pertuzumab, at least indicate the necessity of combination agents to achieve disease remission [62–64]. As we show here, although practically all tumors express HST mRNA, this protein is absent in 75% of breast carcinomas, which indicates that cancer cells are protected by some intrinsic mechanism against the putative growth-inhibitory effects of this molecule. If this negative regulation occurs at the pretranslational level, then it seems possible that exogenous administration of pan-HER antibodies would help block tumor growth. If the protein is produced but excreted from the cells, then it seems possible that the mechanism, which does not allow the endogenous inhibitor to act, will also apply to the exogenous administered antibody as well. Most importantly, if 25% of breast carcinomas grow in the presence of an endogenous pertuzumab-like inhibitor, which is produced in high amounts in some cases with adverse prognostic parameters (HER2 overexpression, activated Akt/PKB, and blocked $p21^{CIP1/WAF1}$), then it remains questionable whether these cancers would benefit from exogenous attempts to disrupt HER2 dimerization. These findings need to be considered in the frame of clinical testing of pan-HER–inhibitory antibodies with similar biologic effects to HST in the experimental setting.

Acknowledgments

The authors thank C. and N. Mitsiades for supplying most of the reagents used in this study. We also thank Emily Daskalaki for excellent technical assistance.

References

[1] Slamon DJ, Clark GM, Wong SG, Levin WJ, Ullrich A, and McGuire WL (1987). Human breast cancer: correlation of relapse and survival with amplification of the HER-2/neu oncogene. *Science* **235**, 177–182.

[2] Hudziak RM, Schlessinger J, and Ullrich A (1987). Increased expression of the putative growth factor receptor p185HER2 causes transformation and tumorigenesis of NIH 3T3 cells. *Proc Natl Acad Sci USA* **84**, 7159–7163.

[3] Hudziak RM, Lewis GD, Winget M, Fendly BM, Shepard HM, and Ullrich A (1989). p185HER2 monoclonal antibody has antiproliferative effects *in vitro* and sensitizes human breast tumor cells to tumor necrosis factor. *Mol Cell Biol* **9**, 1165–1172.

[4] Carter P, Presta L, Gorman CM, Ridgway JB, Henner D, Wong WL, Rowland AM, Kotts C, Carver ME, and Shepard HM (1992). Humanization of an anti-p185HER2 antibody for human cancer therapy. *Proc Natl Acad Sci USA* **89**, 4285–4289.

[5] Baselga J, Perez EA, Pienkowski T, and Bell R (2006). Adjuvant trastuzumab: a milestone in the treatment of HER-2–positive early breast cancer. *Oncologist* **11** (Suppl 1), 4–12.

[6] Piccart-Gebhart MJ, Procter M, Leyland-Jones B, Goldhirsch A, Untch M, Smith I, Gianni L, Baselga J, Bell R, Jackisch C, et al. (2005). Trastuzumab after adjuvant chemotherapy in HER2-positive breast cancer. *N Engl J Med* **353**, 1659–1672.

[7] Slamon D and Pegram M (2001). Rationale for trastuzumab (Herceptin) in adjuvant breast cancer trials. *Semin Oncol* **28**, 13–19.

[8] Bilancia D, Rosati G, Dinota A, Germano D, Romano R, and Manzione L (2007). Lapatinib in breast cancer. *Ann Oncol* **18** (Suppl 6), vi26–vi30.

[9] Engel RH and Kaklamani VG (2007). HER2-positive breast cancer: current and future treatment strategies. *Drugs* **67**, 1329–1341.

[10] Meric-Bernstam F and Hung MC (2006). Advances in targeting human epidermal growth factor receptor-2 signaling for cancer therapy. *Clin Cancer Res* **12**, 6326–6330.

[11] Nahta R, Yu D, Hung MC, Hortobagyi GN, and Esteva FJ (2006). Mechanisms of disease: understanding resistance to HER2-targeted therapy in human breast cancer. *Nat Clin Pract Oncol* **3**, 269–280.

[12] Agus DB, Akita RW, Fox WD, Lewis GD, Higgins B, Pisacane PI, Lofgren JA, Tindell C, Evans DP, Maiese K, et al. (2002). Targeting ligand-activated ErbB2 signaling inhibits breast and prostate tumor growth. *Cancer Cell* **2**, 127–137.

[13] Franklin MC, Carey KD, Vajdos FF, Leahy DJ, de Vos AM, and Sliwkowski MX (2004). Insights into ErbB signaling from the structure of the ErbB2-pertuzumab complex. *Cancer Cell* **5**, 317–328.

[14] Aigner A, Juhl H, Malerczyk C, Tkybusch A, Benz CC, and Czubayko F (2001). Expression of a truncated 100 kDa HER2 splice variant acts as an endogenous inhibitor of tumour cell proliferation. *Oncogene* **20**, 2101–2111.

[15] Doherty JK, Bond C, Jardim A, Adelman JP, and Clinton GM (1999). The HER-2/neu receptor tyrosine kinase gene encodes a secreted autoinhibitor. *Proc Natl Acad Sci USA* **96**, 10869–10874.

[16] Stix G (2006). Blockbuster dreams. *Sci Am* **294**, 60–63.

[17] Hu P, Feng J, Zhou T, Wang J, Jing B, Yu M, Hu M, Zhang X, Shen B, and Guo N (2005). *In vivo* identification of the interaction site of ErbB2 extracellular domain with its autoinhibitor. *J Cell Physiol* **205**, 335–343.

[18] Shamieh LS, Evans AJ, Denton MC, and Clinton GM (2004). Receptor binding specificities of herstatin and its intron 8–encoded domain. *FEBS Lett* **568**, 163–166.

[19] Azios NG, Romero FJ, Denton MC, Doherty JK, and Clinton GM (2001). Expression of herstatin, an autoinhibitor of HER-2/neu, inhibits transactivation of HER-3 by HER-2 and blocks EGF activation of the EGF receptor. *Oncogene* **20**, 5199–5209.

[20] Justman QA and Clinton GM (2002). Herstatin, an autoinhibitor of the human epidermal growth factor receptor 2 tyrosine kinase, modulates epidermal growth factor signaling pathways resulting in growth arrest. *J Biol Chem* **277**, 20618–20624.

[21] Jhabvala-Romero F, Evans A, Guo S, Denton M, and Clinton GM (2003). Herstatin inhibits heregulin-mediated breast cancer cell growth and overcomes tamoxifen resistance in breast cancer cells that overexpress HER-2. *Oncogene* **22**, 8178–8186.

[22] Mullen P, Cameron DA, Hasmann M, Smyth JF, and Langdon SP (2007). Sensitivity to pertuzumab (2C4) in ovarian cancer models: cross-talk with estrogen receptor signaling. *Mol Cancer Ther* **6**, 93–100.

[23] Nahta R, Hung MC, and Esteva FJ (2004). The HER-2–targeting antibodies trastuzumab and pertuzumab synergistically inhibit the survival of breast cancer cells. *Cancer Res* **64**, 2343–2346.

[24] Staverosky JA, Muldoon LL, Guo S, Evans AJ, Neuwelt EA, and Clinton GM (2005). Herstatin, an autoinhibitor of the epidermal growth factor receptor family, blocks the intracranial growth of glioblastoma. *Clin Cancer Res* **11**, 335–340.

[25] Zhou BP, Liao Y, Xia W, Spohn B, Lee MH, and Hung MC (2001). Cytoplasmic localization of $p21^{CIP1/WAF1}$ by Akt-induced phosphorylation in HER-2/neu–overexpressing cells. *Nat Cell Biol* **3**, 245–252.

[26] Kirkegaard T, Witton CJ, McGlynn LM, Tovey SM, Dunne B, Lyon A, and Bartlett JM (2005). AKT activation predicts outcome in breast cancer patients treated with tamoxifen. *J Pathol* **207**, 139–146.

[27] Vestey SB, Sen C, Calder CJ, Perks CM, Pignatelli M, and Winters ZE (2005). Activated Akt expression in breast cancer: correlation with p53, Hdm2 and patient outcome. *Eur J Cancer* **41**, 1017–1025.

[28] Park SS and Kim SW (2007). Activated Akt signaling pathway in invasive ductal carcinoma of the breast: correlation with HER2 overexpression. *Oncol Rep* **18**, 139–143.

[29] Tokunaga E, Kimura Y, Oki E, Ueda N, Futatsugi M, Mashino K, Yamamoto M, Ikebe M, Kakeji Y, Baba H, et al. (2006). Akt is frequently activated in HER2/neu-positive breast cancers and associated with poor prognosis among hormone-treated patients. *Int J Cancer* **118**, 284–289.

[30] Winters ZE, Leek RD, Bradburn MJ, Norbury CJ, and Harris AL (2003). Cytoplasmic $p21^{WAF1/CIP1}$ expression is correlated with HER-2/neu in breast cancer and is an independent predictor of prognosis. *Breast Cancer Res* **5**, R242–R249.

[31] Xia W, Chen JS, Zhou X, Sun PR, Lee DF, Liao Y, Zhou BP, and Hung MC (2004). Phosphorylation/cytoplasmic localization of $p21^{CIP1/WAF1}$ is associated with HER2/neu overexpression and provides a novel combination predictor for poor prognosis in breast cancer patients. *Clin Cancer Res* **10**, 3815–3824.

[32] Finak G, Sadekova S, Pepin F, Hallett M, Meterissian S, Halwani F, Khetani K, Souleimanova M, Zabolotny B, Omeroglu A, et al. (2006). Gene expression signatures of morphologically normal breast tissue identify basal-like tumors. *Breast Cancer Res* **8**, R58.

[33] Scott GK, Robles R, Park JW, Montgomery PA, Daniel J, Holmes WE, Lee J, Keller GA, Li WL, Fendly BM, et al. (1993). A truncated intracellular HER2/neu receptor produced by alternative RNA processing affects growth of human carcinoma cells. *Mol Cell Biol* **13**, 2247–2257.

[34] Livak KJ and Schmittgen TD (2001). Analysis of relative gene expression data using real-time quantitative PCR and the 2(–Delta Delta *C*(T)) method. *Methods* **25**, 402–408.

[35] Bieche I, Onody P, Tozlu S, Driouch K, Vidaud M, and Lidereau R (2003). Prognostic value of ERBB family mRNA expression in breast carcinomas. *Int J Cancer* **106**, 758–765.

[36] Camenisch TD, Schroeder JA, Bradley J, Klewer SE, and McDonald JA (2002). Heart-valve mesenchyme formation is dependent on hyaluronan-augmented activation of ErbB2-ErbB3 receptors. *Nat Med* **8**, 850–855.

[37] Fisher MC, Clinton GM, Maihle NJ, and Dealy CN (2007). Requirement for ErbB2/ErbB signaling in developing cartilage and bone. *Dev Growth Differ* **49**, 503–513.

[38] Ross JS, Fletcher JA, Bloom KJ, Linette GP, Stec J, Symmans WF, Pusztai L, and Hortobagyi GN (2004). Targeted therapy in breast cancer: the HER-2/neu gene and protein. *Mol Cell Proteomics* **3**, 379–398.

[39] Sweeney C, Miller JK, Shattuck DL, and Carraway KL III (2006). ErbB receptor negative regulatory mechanisms: implications in cancer. *Proc Natl Acad Sci USA* **101**, 17138–17143.

[40] Jackson-Fisher AJ, Bellinger G, Ramabhadran R, Morris JK, Lee KF, and Stern DF (2004). ErbB2 is required for ductal morphogenesis of the mammary gland. *Proc Natl Acad Sci USA* **101**, 17138–17143.

[41] Troyer KL and Lee DC (2001). Regulation of mouse mammary gland development and tumorigenesis by the ERBB signaling network. *J Mammary Gland Biol Neoplasia* **6**, 7–21.

[42] Fehm T, Becker S, Duerr-Stoerzer S, Sotlar K, Mueller V, Wallwiener D, Lane N, Solomayer E, and Uhr J (2007). Determination of HER2 status using both serum HER2 levels and circulating tumor cells in patients with recurrent breast cancer whose primary tumor was HER2 negative or of unknown HER2 status. *Breast Cancer Res* **9**, R74.

[43] Fornier MN, Seidman AD, Schwartz MK, Ghani F, Thiel R, Norton L, and Hudis C (2005). Serum HER2 extracellular domain in metastatic breast cancer patients treated with weekly trastuzumab and paclitaxel: association with HER2 status by immunohistochemistry and fluorescence *in situ* hybridization and with response rate. *Ann Oncol* **16**, 234–239.

[44] Muller V, Witzel I, Luck HJ, Kohler G, von Minckwitz G, Mobus V, Sattler D, Wilczak W, Loning T, Janicke F, et al. (2004). Prognostic and predictive impact of the HER-2/neu extracellular domain (ECD) in the serum of patients treated with chemotherapy for metastatic breast cancer. *Breast Cancer Res Treat* **86**, 9–18.

[45] Rampaul RS, Pinder SE, Gullick WJ, Robertson JF, and Ellis IO (2002). HER-2 in breast cancer—methods of detection, clinical significance and future prospects for treatment. *Crit Rev Oncol Hematol* **43**, 231–244.

[46] ADVIA Centaur HER-2/neu Assay [package insert]. Deerfield, IL: Siemens Healthcare Diagnostics Inc.; 2007–2008. Available from: http://diagnostics.siemens.com/webapp/wcs/stores/servlet/PSGenericDisplay~q_catalogId~e_~111~a_langId~e_~111~a_pageId~e_79003~a_storeId~e_10001.htm.

[47] Carney WP, Marks PJ, Mazzara GP, McKenzy SJ, Morgan JH, Petit DA, and Weinberg RA. Detection and quantification of neu related proteins in the biological fluids of humans. International Patent WO/1991/005264. April 18, 1991. OCR text available from: http://www.wipo.int/pctdb/en/wo.jsp?WO=1991%2F05264&IA=WO1991%2F05264&DISPLAY=DESC.

[48] Christianson TA, Doherty JK, Lin YJ, Ramsey EE, Holmes R, Keenan EJ, and Clinton GM (1998). NH2-terminally truncated HER-2/neu protein: relationship with shedding of the extracellular domain and with prognostic factors in breast cancer. *Cancer Res* **58**, 5123–5129.

[49] Cicenas J, Urban P, Vuaroqueaux V, Labuhn M, Kung W, Wight E, Mayhew M, Eppenberger U, and Eppenberger-Castori S (2005). Increased level of phosphorylated Akt measured by chemiluminescence-linked immunosorbent assay is a predictor of poor prognosis in primary breast cancer overexpressing ErbB-2. *Breast Cancer Res* **7**, R394–R401.

[50] Perez-Tenorio G, Berglund F, Esguerra Merca A, Nordenskjold B, Rutqvist LE, Skoog L, and Stal O (2006). Cytoplasmic $p21^{WAF1/CIP1}$ correlates with Akt activation and poor response to tamoxifen in breast cancer. *Int J Oncol* **28**, 1031–1042.

[51] Stal O, Perez-Tenorio G, Akerberg L, Olsson B, Nordenskjold B, Skoog L, and Rutqvist LE (2003). Akt kinases in breast cancer and the results of adjuvant therapy. *Breast Cancer Res* **5**, R37–R44.

[52] Irie HY, Pearline RV, Grueneberg D, Hsia M, Ravichandran P, Kothari N, Natesan S, and Brugge JS (2005). Distinct roles of Akt1 and Akt2 in regulating cell migration and epithelial-mesenchymal transition. *J Cell Biol* **171**, 1023–1034.

[53] Maroulakou IG, Oemler W, Naber SP, and Tsichlis PN (2007). Akt1 ablation inhibits, whereas Akt2 ablation accelerates, the development of mammary adenocarcinomas in mouse mammary tumor virus (MMTV)–ErbB2/neu and MMTV-polyoma middle T transgenic mice. *Cancer Res* **67**, 167–177.

[54] Zinda MJ, Johnson MA, Paul JD, Horn C, Konicek BW, Lu ZH, Sandusky G, Thomas JE, Neubauer BL, Lai MT, et al. (2001). AKT-1, -2, and -3 are expressed in both normal and tumor tissues of the lung, breast, prostate, and colon. *Clin Cancer Res* **7**, 2475–2479.

[55] Liu W, Bagaitkar J, and Watabe K (2007). Roles of AKT signal in breast cancer. *Front Biosci* **12**, 4011–4019.

[56] Yoeli-Lerner M, Yiu GK, Rabinovitz I, Erhardt P, Jauliac S, and Toker A (2005). Akt blocks breast cancer cell motility and invasion through the transcription factor NFAT. *Mol Cell* **20**, 539–550.

[57] Mayo LD and Donner DB (2001). A phosphatidylinositol 3-kinase/Akt pathway promotes translocation of Mdm2 from the cytoplasm to the nucleus. *Proc Natl Acad Sci USA* **98**, 11598–11603.

[58] Schmitz KJ, Grabellus F, Callies R, Wohlschlaeger J, Otterbach F, Kimmig R, Levkau B, Schmid KW, and Baba HA (2006). Relationship and prognostic significance of phospho-(serine 166)–murine double minute 2 and Akt activation in node-negative breast cancer with regard to p53 expression. *Virchows Arch* **448**, 16–23.

[59] Li Q, Mullins SR, Sloane BF, and Mattingly RR (2008). p21-Activated kinase 1 coordinates aberrant cell survival and pericellular proteolysis in a three-dimensional culture model for premalignant progression of human breast cancer. *Neoplasia* **10**, 314–329.

[60] Perera RM, Zoncu R, Johns TG, Pypaert M, Lee FT, Mellman I, Old LJ, Toomre DK, and Scott AM (2007). Internalization, intracellular trafficking, and biodistribution of monoclonal antibody 806: a novel anti-epidermal growth factor receptor antibody. *Neoplasia* **9**, 1099–1110.

[61] Shepard HM, Jin P, Slamon DJ, Pirot Z, and Maneval DC (2008). Herceptin. *Handb Exp Pharmacol* (181), 183–219.

[62] Agus DB, Sweeney CJ, Morris MJ, Mendelson DS, McNeel DG, Ahmann FR, Wang J, Derynck MK, Ng K, Lyons B, et al. (2007). Efficacy and safety of single-agent pertuzumab (rhuMAb 2C4), a human epidermal growth factor receptor dimerization inhibitor, in castration-resistant prostate cancer after progression from taxane-based therapy. *J Clin Oncol* **25**, 675–681.

[63] Attard G, Kitzen J, Blagden SP, Fong PC, Pronk LC, Zhi J, Zugmaier G, Verweij J, de Bono JS, and de Jonge M (2007). A phase Ib study of pertuzumab, a recombinant humanised antibody to HER2, and docetaxel in patients with advanced solid tumours. *Br J Cancer* **97**, 1338–1343.

[64] Herbst RS, Davies AM, Natale RB, Dang TP, Schiller JH, Garland LL, Miller VA, Mendelson D, Van den Abbeele AD, Melenevsky Y, et al. (2007). Efficacy and safety of single-agent pertuzumab, a human epidermal receptor dimerization inhibitor, in patients with non small cell lung cancer. *Clin Cancer Res* **13**, 6175–6181.